

## Study on Anodic Oxidation and Sealing of Aluminum Alloy

Ye Wan<sup>\*</sup>, Huan Wang, Yundian Zhang, Xiumei Wang, Yanbo Li

School of Materials Science and Engineering, Shenyang Jianzhu University, Shenyang 110168, China

\*E-mail: [ywan@sjzu.edu.cn](mailto:ywan@sjzu.edu.cn)

*Received:* 9 October 2017 / *Accepted:* 15 December 2017 / *Published:* 28 December 2017

---

Alumina films were prepared on the surfaces of 2024 aluminum alloy by the anodic oxidation, the sealing and the coloring methods. The films were studied via scanning electron microscopy, X-ray diffraction, the surface roughness, the indentation hardness, the abrasion resistance and the corrosion resistance tests. The results revealed that porous alumina was detected on the surface of the aluminum alloy samples after the anodic oxidation treatment and the amount of the pores decreased with the oxidation time. The anodic oxidation film became denser with the oxidation time and enhanced the corrosion resistance of 2024 aluminum alloy. The anodic oxidation process decreased the surface roughness of aluminum alloy. The samples' hardness, abrasion resistance and corrosion resistance were increased by the sealing process for the anodic oxidation films. The combination procedure of anodic oxidation and sealing with boiling water improved the hardness and the abrasion resistance of the samples greatly.

---

**Keywords:** Aluminum alloy; Anodic oxidation; Alumina film; Sealing; Performance test

### 1. INTRODUCTION

Owing to the remarkable combination of characteristics, such as low density, easy workability, superior corrosion resistance, and high electric/heat conductivity [1], aluminum and its alloys have already broadly and deeply used in aerospace, transportation, communications equipment, and many other aspects[2-3]. For example, the AA2XXX (Al-Cu) alloys are widely employed for aerospace applications because of their excellent specific mechanical properties, damage tolerance and low density [4]. However, the poor corrosion resistance and abrasion resistance are the main factors which restrict widely application of aluminum alloys. Aluminum alloys and their structural integrity become susceptible to different forms of corrosion such as stress corrosion cracking, pitting corrosion and inter granular corrosion, especially in chloride environment [5-9].

It was well known that a natural oxide film could be formed on the surfaces of aluminum alloy in the natural environments. Unlike the protective films of other alloys, the films of aluminum alloys

are easily damaged in the extreme environments, such as acid rain, industrial dust and the greenhouse atmospheres. Aluminum alloys have poor weather ability and reliability because of the loose and porous structures of the film on the surfaces. The porous film influences corrosion resistance and usage of aluminum and its alloy greatly. Thus many efforts have been made to improve the wear resistance and corrosion resistance of aluminum alloys as well. For example, there was great attention in order to study corrosion protection with the goal of extending the lifetime of metal and metal alloy objects [10]. Many surface modification technologies were developed rapidly to enhance the performances of aluminum alloys. The surface modification technologies of aluminum alloy mainly include anodic oxidation, chemical oxidation, coating, electroplating [11-13] and relate with metallography, chemistry, electrochemistry, material production technology and other disciplines. Anodic oxidation, one of the important surface modification methods, was often used to prepare oxide films for aluminum alloys and has the most rapid and versatile application among those technologies [14]. As the pore size and the thickness can be controlled by anodic oxidation, the oxide film can be used as a kind of good template material and obtains a wide range of applications in the synthesis of ordered nanostructures [15-17].

The electrolysis process including formation and dissolution of the film are occurred at the same time during the aluminum anodic oxidation. Many pores are formed on the surface of aluminum alloy during the process. Sealing technology is necessary [18-19] to improve corrosion resistance of aluminum alloys because anodic aluminum films are porous. The purpose of this paper is to enhance hardness, abrasion resistance and corrosion resistance of the surface of 2024 aluminum alloy via the anodic oxidation and sealing procedure. The aluminum alloy is polarized under periodic anodization voltage in the sulfuric acid solution. Porous films were formed on the surfaces of 2024 aluminum alloy polarized by anodic oxidation, which parameters influenced the morphologies and properties of the anodic oxide films. The anodic alumina membrane is tailored via the potentiostatic method by varying anodization parameters including time, voltage and current. The microstructure of the film was observed and detected by scanning electron microscopy and X-ray diffraction. The performances of the oxidation films were examined. The reaction mechanisms were considered in this paper as well.

## **2. EXPERIMENTAL**

### *2.1 Pretreatment of 2024 aluminum alloy*

2024 aluminum alloy specimen with the size of 10mm × 10mm × 5mm were wet polished with a series of SiC papers of 240, 600 and 1200 grits, and then degreased with alcohol and rinsed with deionized water prior to anodic oxidation and electrochemical test.

### *2.2 Film preparation*

The anodic oxidation of aluminum alloy was performed via the potentiostatic method with a LK3200A (Lanlike Co. Ltd., CN) electrochemical instrument at 25°C. A three electrode cell exposed

a 1 cm<sup>2</sup> portion of the samples to be work electrode. A flat platinum wire mesh was served as a counter electrode and a saturated calomel electrode as a reference electrode. All potentials were measured against the saturated calomel electrode and quoted against this scale. The electrolyte solution for anodic oxidation was made by the mixture of sulfuric acid solution (184g/L) and aluminum sulfate solution (20g/L). The anodic oxidation times were 4000 s, 8000 s, 10000 s and 12000 s respectively.

Two kinds of solutions were used to seal the porous films of anodic oxidation. One was the sealing process by immersing the anodic oxidized samples in boiling water for 30, and the other was immersing the anodic oxidized samples in the nickel sulfate solution (the concentration is 8g/L) for 20 min at the temperature of 85°C - 95°C.

### 2.3 Surface examination

After surface treatment, the films of aluminum alloy were explored with many methods. The images of the specimens were observed by scanning electron microscopy (SEM) (s-4800, Hitachi, Japan). The structures of the samples were identified with an X-ray diffraction (XRD) (D/max-2400, Rigaku, Japan) with Cu K $\alpha$  radiation. Surface roughness of the aluminum samples was examined using a profilometer (Surtronic25, Taylor-Hobson, UK). The HV-1000 tester (HV-1000, Lianer, China) with a 10Moons SDK2000<sup>®</sup> software recorder was used to measure the indentation hardness of the aluminum surfaces. All the films were loaded with a 0.490 N test force for about 15s during the indentation hardness measurement. Corrosion resistance was characterized by spot tests. A polishing equipment with 240 grits SiC paper on the abrasive disk was applied to detect the abrasion resistance of the alumina film. In this way, the oxidized faces of the samples were evenly pressed 5 minutes with a constant force on the abrasive disk rotating with 300 rpm and wetted by a tiny stream. The mass losses of the samples after the abrasion were used for the evaluation of film abrasion resistance.

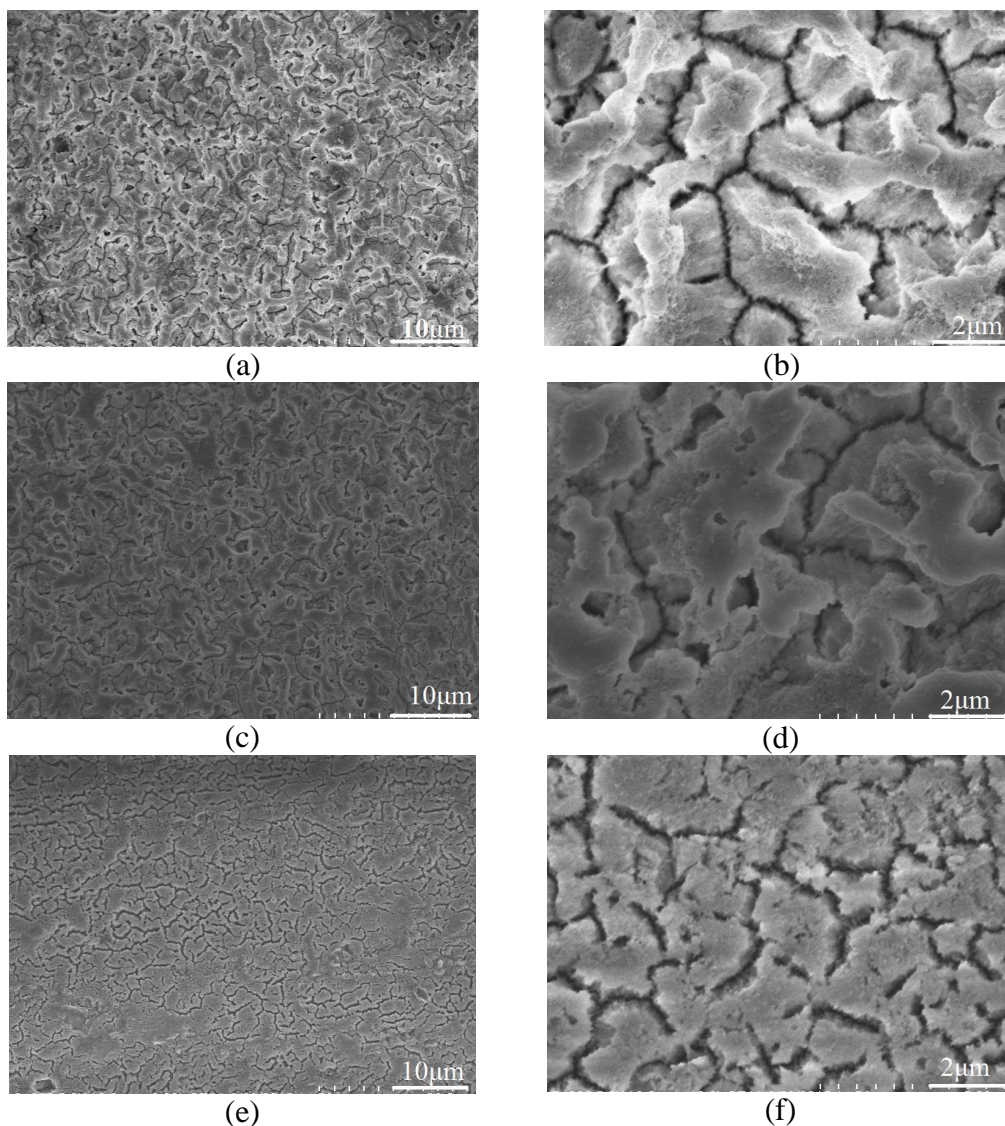
## 3. RESULTS AND DISCUSSION

### 3.1 Surface images of the films

Fig.1 is the SEM images of the aluminum surfaces oxidized for different time by the single-potential step chronoamperometry mode with a 10V potential step. It is clear that the samples were coated a film evenly by the anodic oxidation procedure. There were some irregular apertures on the surface of the aluminum samples after oxidized for 8000s, seen in Fig. 1(a) and (b). The apertures distributed evenly on the surfaces of the samples. The cracks with the size about 10  $\mu$ m were formed on the outer oxidation layer of film.

After anodic oxidization for 12000s, there were barely apertures on the surface of the oxidized aluminum samples, seen in Fig. 1(e) and (f). Fig. 1 also shows that the apertures interpenetrated with each other and agglomerated together to form the cracks with the oxidation process going on. The cracks began to shorten progressively and their sizes were approximately 5 $\mu$ m after the samples being

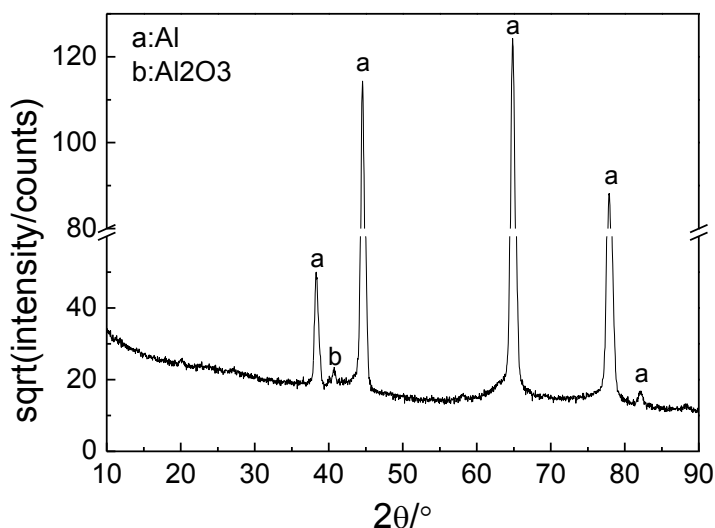
oxidized 12000s. The films became more compact and the amounts of the apertures and the cracks were less with oxidation time prolonging.



**Figure 1.** Low- and high-magnification SEM images of aluminum anodic oxidized with the single-potential step chronoamperometry mode. The oxidation times are 8000s (a) and (b), 10000s (c) and (d), 12000s (e) and (f) respectively. The step of the potential is 10V.

### 3.2 Microstructure of the films

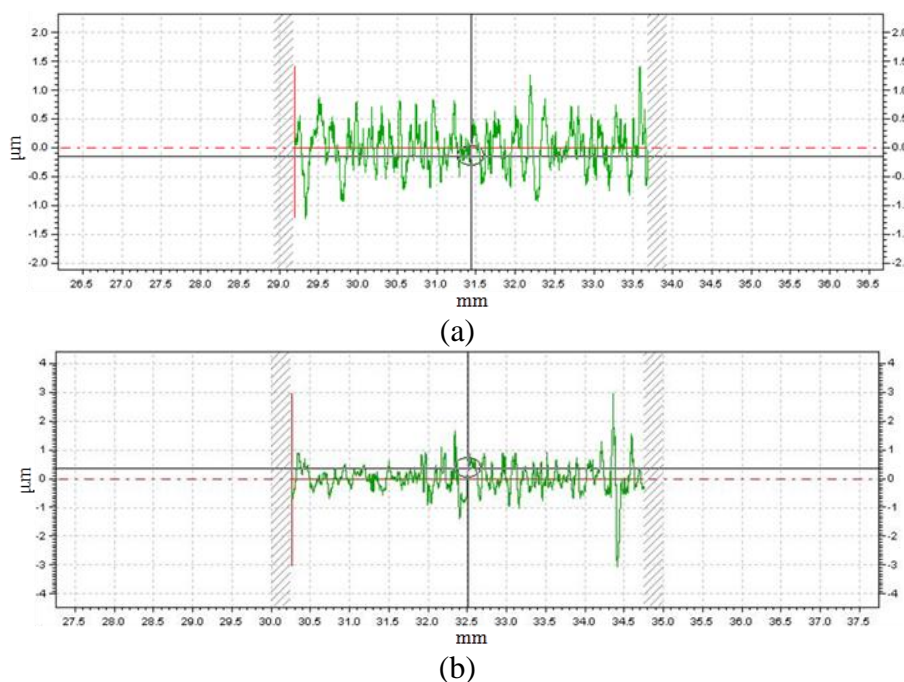
In order to study the film structure, the anodic oxidized aluminum surface was analyzed by the XRD method. Fig. 2 is the X-ray diffraction pattern of the film of the aluminum sample oxidized for 10000s. The diffraction peak that  $2\theta$  was about  $40.64^\circ$  was attributed to  $\theta\text{-Al}_2\text{O}_3$ , which always co-exists with  $\gamma\text{-Al}_2\text{O}_3$  and  $\alpha\text{-Al}_2\text{O}_3$  [19]. The series of peaks that  $2\theta$  was approximately  $38.1^\circ$ ,  $44.3^\circ$ ,  $64.4^\circ$  and  $77.4^\circ$  belonged to crystal faces of (111), (200), (220) and (311) of metallic Al respectively. The intensities of the diffraction peaks of aluminum substrate were stronger than those of aluminum oxide, owing to that the anodic oxidation film was thin and X-rays pierced through into the substrate.



**Figure 2.** XRD pattern of the specimen surface after anodic oxidation for 10000s with a single constant step chronoamperometry mode.

### 3.3 Surface roughness of the films

Fig. 3 shows surface roughness of the aluminum samples after anodic oxidation for different time. Table 1 lists  $S_R$  (the value of surface roughness) extracted from Fig. 3 by the profilometer. It can be seen from Table 1 that  $S_R$  of every sample is small, which indicates the surfaces were smooth and were aesthetic and convenient for further treatment, for example coloring. The data in Table 1 and Fig. 3 indicated  $S_R$  decreased with the anodic oxidation time. The surface of aluminum oxide becomes smoother and smoother with oxidation time increasing.



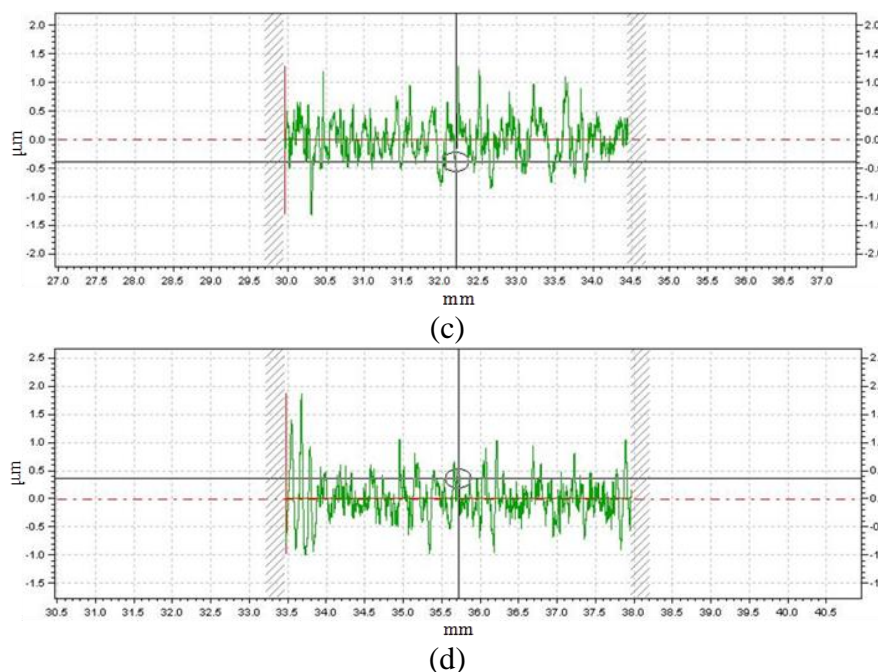


**Figure 3.** Surface roughness of the aluminum samples after anodic oxidation for different time, (a) 4000s, (b) 8000s, (c) 10000s, (d) 12000s.

**Table 1.**  $S_R$  of the samples after anodic oxidation.

Time of anodic oxidation (s)	$S_R$ ( $\mu\text{m}$ )
4000	0.3451
8000	0.3039
10000	0.2788
12000	0.2745

### 3.4 Indentation hardness of the films

Fig. 4 shows diamond indentation on the surfaces of the samples. The indentation depth in Fig. 4 was used to illustrate indentation hardness of the samples. It can be seen from Fig. 4 that there is no crack or exfoliation on the surfaces of the samples after the indentation hardness test. The values of the surface indentation hardness of anodic oxide film was extracted automatically by the software of the indentation hardness tester and showed in Table 2. Surface hardness increased approximately 23.4% after the anodic oxidation treatment. The method sealing the porous alumina with boiling water improved the surface hardness of the films significantly. Surface hardness of the samples was improved by sealing the porous samples with nickel sulfate as well, but not so much as that with boiling water. After anodic oxidation, some samples were colored to be red. According to Fig. 4 and Table 2, the coloring method didn't improve indentation hardness of the films further, which was different with the sealing process.

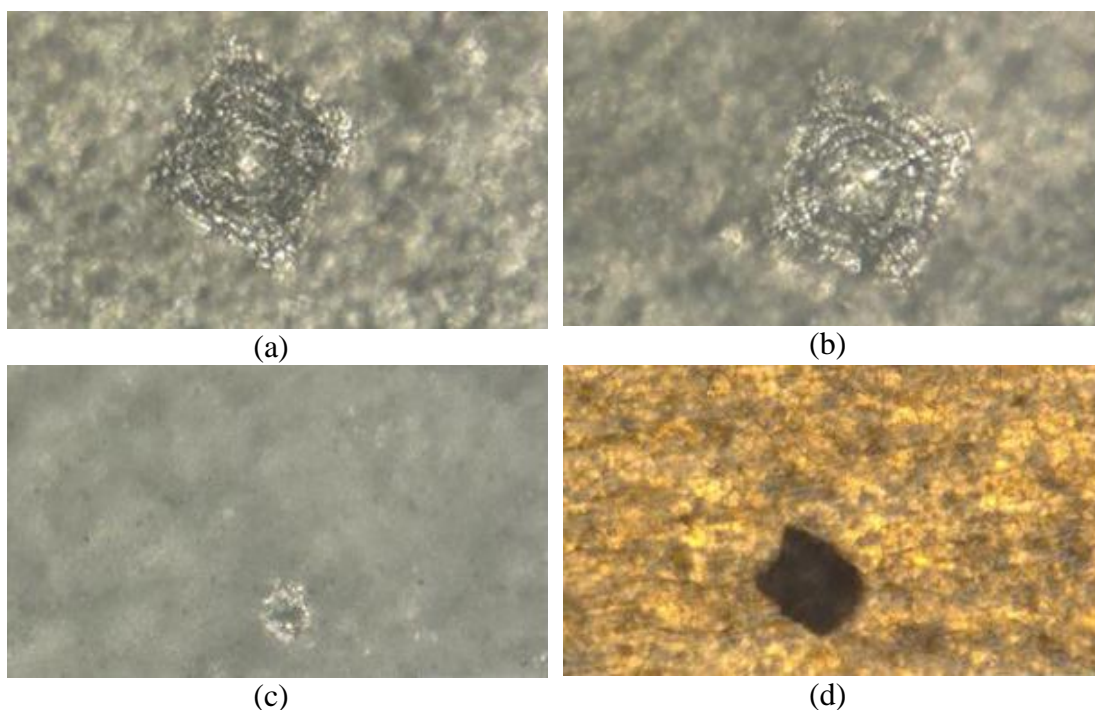


**Figure 4.** Images of the aluminum samples after the indentation hardness test. (a), (b), (c) and (d) are the anodic oxidized samples and not sealed, sealed with boiling water, sealed with NiSO<sub>4</sub> solution, and reddened respectively.

**Table 2.** Indentation hardness of the aluminum samples.

Aluminum samples	Indentation hardness
Blank	131
Oxidized and not sealed	161.6
Oxidized and sealed with boiling water	172.4
Oxidized and sealed with NiSO <sub>4</sub> solution	145
Oxidized and reddened	162.2

### 3.5 Abrasion resistance of the films

After the aluminum samples modified by the different means, the films were analyzed with the goal of testing abrasion resistance by a polishing method. Compared to the sand trickling test, the polishing abrasion test shows the surface remains relatively smooth and a continuous abrasion occurs though the film [21]. Therefore, it was decided that the polishing abrasion test was used to measure the mass loss directly. The abrasion resistance test is based on the mass loss of each sample after polishing. The mass of the samples after abrasion for different time is shown in Table 3. The data given here in Fig. 5 are examples of a continuous abrasion, or “polishing” of the top layer. “Blank” in Fig. 5 means the samples wasn’t anodic oxidized, sealed or colored. It can be seen from Table 3 and

Fig. 5 that the mass loss of the blank sample was the biggest, followed by the samples oxidized and not sealed, the samples oxidized and redden, the samples oxidized and sealed with boiling water. After 20 minutes' polishing, the percentage of mass loss is 32.8% for the blank sample, 0.97% for the anodic oxidized and not sealed sample, 0.46% for the anodic oxidized and redden sample, 0.4% for the anodic oxidized and sealed with boiling water.

**Table 3.** Mass of the samples after polishing different time (g).

Polishing time, min	Blank	Oxidized and not sealed	Oxidized and sealed with boiling water	Oxidized and redden
0	4.8037	4.6711	4.5757	4.7261
5	4.76	4.6585	4.5708	4.7155
10	4.7264	4.6355	4.5685	4.7133
15	4.6699	4.6322	4.5681	4.7112
20	4.6463	4.6259	4.5566	4.7042

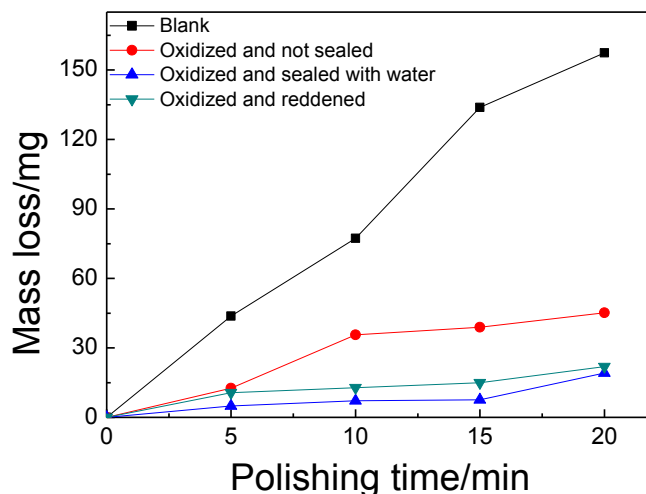


**Figure 5.** Mass loss of the different samples after being polished different time.

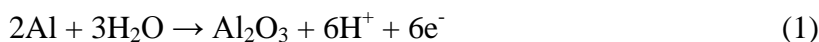
### 3.6 Corrosion resistance of the films

The spot tests with the acid and the alkali solutions were used on the purpose of estimating corrosion resistance of the films of anodic oxidized aluminum. A drop of a 3(wt.%) sulfuric acid solution and a 3(wt.%) sodium hydroxide solution was put on the surfaces of the samples respectively to measure corrosion resistance of the films. The time from dripping the solution on the surface to generating bubbles was used to assess corrosion resistance of the alumina films. Table 4 lists the time started to generate bubbles for the aluminum samples. No bubble appears on the surfaces of the samples after dripping the sulfate solution 3 minutes, or dripping the alkali solution 1 minute.

**Table 4.** Time starting to generate bubbles after dripping the solutions on the samples

	Oxidized and not sealed	Oxidized and sealed with boiling water	Oxidized and sealed with NiSO <sub>4</sub> solution
3% sulfuric acid solution	>3min	>3min	>3min
3% sodium hydroxide solution	80s	110s	100s

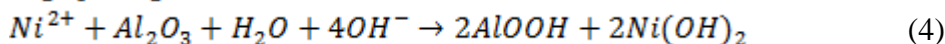
During the anodic oxidation procedure, both formation and dissolution of oxide film occurred on the surfaces of the aluminum samples at the same time [20]. Film-formation arose according to Reaction (1) and film-dissolving according to Reaction (2). Al<sup>3+</sup> escaped from substrate through the interface of metal/oxide and migrated into the oxide film, while O<sup>2-</sup> was generated at the interface of the electrolyte solution/metal and moved in the opposite direction of Al<sup>3+</sup>. Once Al<sup>3+</sup> met O<sup>2-</sup>, the oxide film was formed.



Based on the mechanism of Reaction (1), some Al<sub>2</sub>O<sub>3</sub> of the alumina film was dissolved and pores were formed on the surfaces of the samples. When the electrolyte solution permeated through the pores, new aluminum oxides were formed again. Alumina films grew and then gradually extended into further inner substrate relying on the formation and the growth of the porous layer [22].

Fig. 1 shows there were many cracks on the surfaces of the oxidized samples. One probable reason for crack formation is that stress arose in the film by anodic oxidation. After a certain elapsed time, the film fracture appeared and crack grew on the surfaces of the samples. The second reason for crack is probably because local corrosion and inter-crystalline corrosion were easy to occur on 2024 aluminum alloy due to Al<sub>2</sub>Cu phase in 2024 aluminum alloy. Not only manganese and iron are rapidly dissolved, but also the copper-rich intermetallic phases were local attacked [23]. After anodic oxidation for 10000s, there was barely crack or exfoliation on the surfaces of the aluminum films, which demonstrates that the films were thickened and the pits were covered by the new formed oxides, seen in Fig. 1.

The third possible reason for the cracks on the surface of the sample is the volume of the alumina expands [24] owing to the anodic oxidation and the sealing. The probably sealing mechanisms of water sealing and nickel sulfate sealing were shown in the following reactions (3) and (4). Reaction (3) indicates the sealing mechanism of hydrothermal sealing [25]. The results in Fig. 4 and Table 2 indicated that boiling water sealing decreased pore size and increased the hardness of the aluminum sample, which is consistent with the Hu's results [26]. For the sealing process with nickel sulfate solution, Ni(OH)<sub>2</sub> was formed on the anodic porous alumina as well. When pH was adjusted to be more than 7, Al(OH)<sub>3</sub> is formed as AlOOH onto the surface of anodic alumina film including the pores. The sealing procedure through the reaction mechanisms described in Reaction (3) and Reaction (4) resulted in improving chemical and mechanical properties of the aluminum alloys [27], which is consistent with the our findings in Fig. 4 and Table 2.



Mass loss of the samples with anodic oxidation and sealing was the smallest, and the oxidized samples with coloring treatment took the second place. The smallest mass loss indicated that the combination of anodic oxidation and sealing improved surface resistance greatly. During the coloring process, the organic dye molecules diffused into the pores and densified the porous alumina, which improved surface abrasion resistance and reduced the mass loss of the aluminum alloy to a certain degree.

#### 4. CONCLUSION

The present work deals with the surface treatment of 2024 aluminum alloy. The effects of the anodic oxidation, sealing and coloring on the properties of the oxide films have been studied and compared using many methods. Anodic oxidation was performed in sulfuric acid with a potentiostatic method. After anodic oxidation, the film was mainly made of the crystalline porous  $\theta$ - $Al_2O_3$ . The surface roughness data shows that the sample's surface became smoother after anodic oxidation. The anodic oxidation film became denser and more compact in the sulfuric acid solution, and the amounts of the apertures and the cracks were less with oxidization time prolonging. The results of indentation hardness indicated that the anode oxidation treatment improved the surface hardness of aluminum alloy significantly. In addition, the boiling water sealing process made a further improvement to the hardness as well, while coloring had barely influence on the film's hardness. Both of the results from abrasion resistance and corrosion resistance tests demonstrated that the anodic oxidation treatment and the sealing treatment improved the abrasion resistance and corrosion resistance of the surface of 2024 aluminum alloy to some extent.

#### ACKNOWLEDGEMENTS

The authors gratefully appreciate the financial support from by Liaoning Natural Science Foundation (Grant No.: 2015020227) and Program for Changjiang Scholars and Innovative Research Team in University of Ministry of Education of China (Grant No.: IRT\_15R45).

#### References

1. K.A. Yasakau, M.L. Zheludkevich and M.G.S. Ferreira, *Intermetallic Matrix Composites*, Woodhead Publishing, (2018) 425.
2. Z.F. Zhu, *Technology of anodic oxidation and treatment on aluminum alloys*, 2nd edition, Beijing: Chemical Industry Press, 2010.
3. A. Heinz, A. Haszler, C. Keidel, S. Moldenhauer, R. Benedictus and W. S. Miller, *Mater. Sci. Eng. A*, 280(1) (2000) 102.
4. D. Embuka, A.E. Coy, C.A. Hernandez-Barrios, F. Viejo, and Z. Liu, *Surf. Coat. Technol.*, 313 (2017) 214.
5. M. Trueba and S.P. Trasatti, *Mater. Chem. Phys.*, 121 (3) (2010) 523.

6. V. Pandey, J.K. Singh, K. Chattopadhyay, N.C. Santhi Srinivas and V. Singh, *J. Alloys Compd.*, 723 (2017) 826.
7. T.M. Yue, L.J. Yan and C.P. Chan, *Appl. Surf. Sci.*, 252 (2006) 5026.
8. B. Priet, G. Odemer, C. Blanc, K. Giffard and L. Arurault, *Surf. Coat. Technol.*, 307 (2016) 206.
9. C. Augustin, E. Andrieu, C. Blanc, J. Delfosse and G. Odemer, *J. Electrochem. Soc.*, 157 (2010) 428.
10. R.M. Bandeira, J. van Druenen, A.C. Garcia and G.T. Filho, *Electrochim. Acta*, 240 (2017) 215.
11. C. Lee, K. Oh, D. Lee, Y. Kim and J. Choi, *J. Phys. Chem. Solids*, 103 (2017) 87.
12. E.V. Bryuzgin, V.V. Klimov, S.A. Repin, A.V. Navrotsky and I.A. Novakov, *Appl. Surf. Sci.*, 419 (2017) 454.
13. S.M. Li, S.Z. Zhou and J.H. Liu, *Acta Phys. Chim. Sin.*, 25 (12) (2009) 2581.
14. D.J. Kong and J.C. Wang, *J. Alloys Compd.*, 632(25) (2015) 286.
15. Y. Qi, Y. Zhang and L. Hu, *J. Mater. Eng.*, 2(2) (2013) 17.
16. C. Jeong and C.H. Choi, *ACS Appl. Mater. Interfaces*, 4(2) (2012) 842.
17. C.R. Martin, *Science*, 266(5193) (1994) 1961.
18. F. Mansfeld, C. Chen, C.B. Breslin and D. Dull, *J. Electrochem. Soc.*, 145 (1998) 2792.
19. Y. Zuo, P.H. Zhao and J.M. Zhao, *Surf. Coat. Technol.*, 166 (2003) 237.
20. A. Kumar, A. Kanta, N. Birbilis, T. Williams and B.C. Muddle, *J. Electrochem. Soc.*, 157 (2010) C346.
21. S. Bruns, M. Vergöhl, T. Zickenrott and G. Bräuer, *Surf. Coat. Technol.*, 290(11) (2016):10.
22. C.K. Chung, M.W. Liao, H.C. Chang and C.T. Lee, *Thin Solid Films*, 520(5) (2011) 1554.
23. M. Schneider, T. Liebmann, U. Langklotz and A. Michaelis, *Electrochim. Acta*, 249 (2017) 198.
24. S. Akiya, T. Kikuchi, S. Natsui and R.O. Suzuki, *Appl. Surf. Sci.*, 403 (2017) 652.
25. L. Li, Y. Zhang, J. Lei, J. He, R. Lv, N. Li and F. Pan, *Chem. Commun.*, 50 (2014) 7416.
26. N.P. Hu, X.C. Dong, X.Y. He, J.F. Browning and D.W. Schaefer, *Corros. Sci.*, 97 (2015) 17.
27. M. Kim, H.k Yoo and J. Choi, *Surf. Coat. Technol.*, 310 (2017) 106.

© 2018 The Authors. Published by ESG ([www.electrochemsci.org](http://www.electrochemsci.org)). This article is an open access article distributed under the terms and conditions of the Creative Commons Attribution license (<http://creativecommons.org/licenses/by/4.0/>).